

Title	Hydrothermal Synthesis and Morphology Control of TiO <sub>2</sub> Nanocrystals
Author(s)	Tan, Zhenquan; Yamamoto, Kazuhiro; Qiu, Nan et al.
Citation	Transactions of JWRI. 2014, 43(1), p. 21-24
Version Type	VoR
URL	<a href="https://doi.org/10.18910/50963">https://doi.org/10.18910/50963</a>
rights	
Note	

***Osaka University Knowledge Archive : OUKA***

<https://ir.library.osaka-u.ac.jp/>

Osaka University

# Hydrothermal Synthesis and Morphology Control of TiO<sub>2</sub> Nanocrystals<sup>†</sup>

TAN Zhenquan\*, YAMAMOTO Kazuhiro\*, QIU Nan\*, OHARA Satoshi\*\*

## Abstract

*Tailor-made TiO<sub>2</sub> nanocrystals with well-defined exposed facets have attracted increasing research interest recently. The exposed facets greatly determine the reactive activity of TiO<sub>2</sub> nanocrystals and dominate their application potential. Size-controllable TiO<sub>2</sub> nanosheets with highly reactive {001} facets were synthesized by a conventional hydrothermal synthesis process. The particle sizes ranged from 25 nm to several micrometres and a tuneable percentage of {001} surface area ranged from 50 % to 90 % according to the particle size. TiO<sub>2</sub> single crystal and higher-level mesoscopic assemblies with {001} facets, and TiO<sub>2</sub> hollow microspheres were successfully synthesized by the modified hydrothermal approaches in this study.*

**KEY WORDS: (TiO<sub>2</sub>), (nanocrystals), (hydrothermal synthesis), (morphology control), (size control)**

## 1. Introduction

TiO<sub>2</sub> is one of the most studied oxide materials and has been widely used in photocatalysis, catalysis, dye-sensitive solar cells, Li-ion batteries, and in many other applications<sup>1,2</sup>. The physical and chemical properties of TiO<sub>2</sub> closely related to the phase, the size and the shape. For example, the band gap of TiO<sub>2</sub> is determined by the crystalline phase. For anatase TiO<sub>2</sub>, the value is 3.2 eV, which is 0.2 eV larger than that of rutile TiO<sub>2</sub>. On the other hand, the {001} facet of anatase TiO<sub>2</sub> is more reactive than the {101} facet<sup>3</sup>, which promises a use in high-performance photocatalytic applications<sup>4,5</sup>. A tailored-made TiO<sub>2</sub> having strict boundary for {001} and {101} surfaces is greatly helpful for the space-induced electron-hole separation<sup>6</sup>. Additionally, the photocatalytic activity of TiO<sub>2</sub> also partially depends on particle size<sup>7</sup>. Small size offers a large surface area for light absorption and numerous active sites for photocatalytic reaction. A particle size of 25 to 40 nm was suggested for the optimum photocatalytic activity of TiO<sub>2</sub><sup>8</sup>. Therefore, controlling both the size and morphology of nanostructured TiO<sub>2</sub> has currently attracted significant interest among chemists and materials scientists.

Recently we reported the synthesis of the size-controlled TiO<sub>2</sub> nanocrystals with highly exposed {001} facets by a conventional hydrothermal synthesis method<sup>9</sup>. Fluorine-tailoring synthesis is found to be most effective to protect the {001} surfaces during the crystal

growth. In order to avoid the high safety risk of hydrofluoric acid that is generally used as a fluorine-containing tailoring materials<sup>4</sup>, we selected a minimally toxic reagent, ammonium hexafluorotitanate, as an F<sup>-</sup> ion source to synthesize TiO<sub>2</sub> nanocrystals by the hydrothermal method. Another reagent, titanium(IV) butoxide, was used as a Ti source to adjust the F/Ti molar ratio. By carefully adjusting the F/Ti molar ratio, we succeeded in controlling the particle size and tuning the percentage of {001} surface area of TiO<sub>2</sub> nanocrystals. In this paper, we focus on the size and morphology control of anatase TiO<sub>2</sub> nanocrystals synthesized by the hydrothermal approach. We report the size- and morphology-control of nanostructured TiO<sub>2</sub>, including in regular nanosheets, highly-level mesoscopic microspheres assembly, and hollow mesoscopic microspheres.

## 2. Experimental

The hydrothermal method has been widely used to synthesize TiO<sub>2</sub> nanocrystals. Tailor-made TiO<sub>2</sub> nanocrystals are easily synthesized by carefully selecting the hydrothermal conditions such as temperature, reaction time, reactant concentration and capping agents. A general approach to synthesize size and shape controlled TiO<sub>2</sub> nanocrystals with highly exposed {001} facets is described as follows. 1 g of ammonium hexafluorotitanate (99.99% purity) was dissolved into 10 ml of hydrochloric acid (5 M). 6.8 ml of titanium(IV)

<sup>†</sup> Received on June 30, 2014

\* Specially Appointed Researcher

\*\* Associate Professor

Transactions of JWRI is published by Joining and Welding Research Institute, Osaka University, Ibaraki, Osaka 567-0047, Japan

## Hydrothermal Synthesis and Morphology Control of TiO<sub>2</sub> Nanocrystals

butoxide (97% purity) was added to ammonium hexafluorotitanate solution by stirring in a controlled amount such that the total F/Ti molar ratio was 1.2. The mixtures turned to white thickened gels under continuous stirring. The gels were placed into a 50 ml sealed Teflon tube for a 6-hour hydrothermal reaction at 180 °C. The products were washed with ultrapure water (18.2 MΩ) three times and by methanol once, all with subsequent centrifugal separation (10,000 G, 10 min). Finally the products were dried at 50 °C in the ambient atmosphere. The F/Ti ratio, i.e., the total concentration of Ti source, is a key parameter to determine the particle size of as-synthesized TiO<sub>2</sub> nanocrystals.

### 3. Results and Discussion

#### 3.1 Synthesis and size control of TiO<sub>2</sub> nanocrystals having exposed {001} facet

**Figure 1a** shows a typical transmission electron microscopy (TEM) photograph of as-synthesized TiO<sub>2</sub> nanocrystals with an F/Ti ratio of 1.2. X-ray diffraction (XRD) confirmed the anatase crystalline phase for these as-synthesized TiO<sub>2</sub> nanocrystals. The as-synthesized TiO<sub>2</sub> nanocrystals show a regular square shape, which is the apparent {001} surface of the anatase TiO<sub>2</sub> nanocrystals (**Fig. 1b**). **Figure 1c** shows a high-resolution TEM photograph of the {001} facet of as-synthesized TiO<sub>2</sub> nanocrystals. The [001] atomic planes with lattice spacing of 0.19 nm are clearly observed. **Figure 1d** show many rod shaped TiO<sub>2</sub> nanocrystals, which are identified in side-view, i.e., the apparent {101} facet of the anatase TiO<sub>2</sub> nanocrystals. On the high-resolution TEM photograph, it is clearly observed that the [101] and [004] atomic planes have lattice spacings of 0.35 and 0.24 nm, respectively.

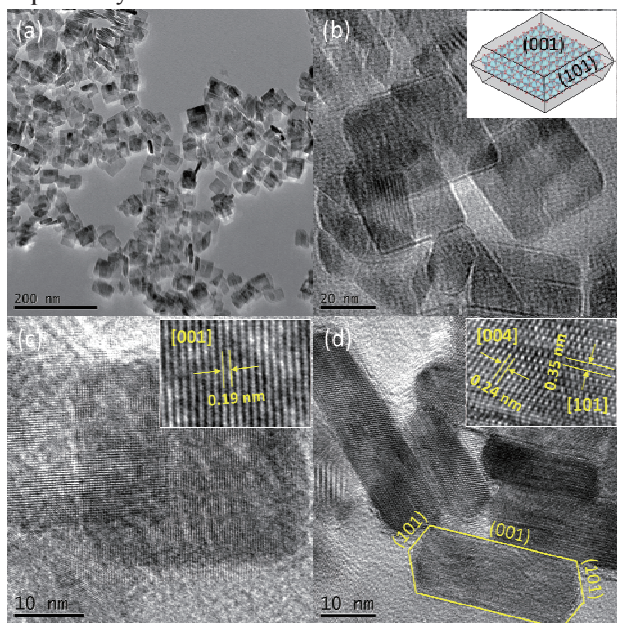


**Fig. 1** TEM photographs of TiO<sub>2</sub> nanocrystals with exposed {001} facets (a, b). Inset in (b) shows a model of TiO<sub>2</sub> nanocrystal with exposed {001} facets. High-resolution TEM photographs for {001} facet (c) and {101} facet (d) of anatase TiO<sub>2</sub> nanocrystals.

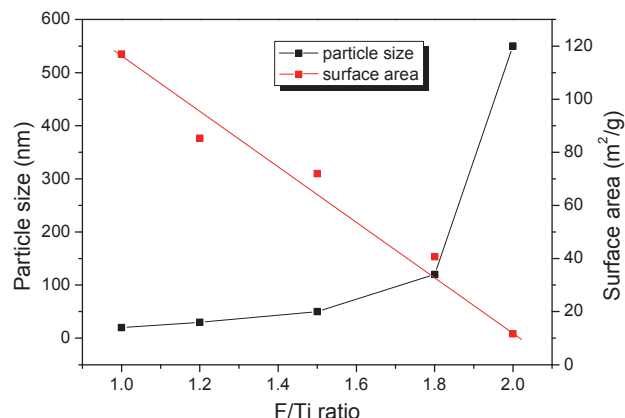


**Fig. 2** Particle size (black dots) and surface area (red dots) of TiO<sub>2</sub> nanocrystals having exposed {001} facets prepared in conditions with various F/Ti ratio.

The size of as-synthesized TiO<sub>2</sub> nanocrystals is easily controlled by the concentration of the Ti source (from both of ammonium hexafluorotitanate and titanium(IV) butoxide). In the formation of exposed {001} facets, F<sup>-</sup> element was used to protect the bare {001} facet in the crystal growth process. The F/Ti ratio is thus an important parameter for shape- and size-control. **Figure 2** shows the relationship between the particle size of as-synthesized TiO<sub>2</sub> nanocrystals and the F/Ti ratio. The average size is 20, 30, 50, 120, and 550 nm, according to the F/Ti ratios of 1.0, 1.2, 1.5, 1.8, and 2.0, respectively. The BET specific surface area of as-synthesized TiO<sub>2</sub> nanocrystals suggests an approximately linear relationship between the specific surface area and the F/Ti ratio.

#### 3.2 TiO<sub>2</sub> single crystals having exposed {001} facet

Using a similar hydrothermal process only with some modified parameters, we easily synthesized micrometre-sized anatase TiO<sub>2</sub> single crystals with exposed {001} facets. An important parameter was total concentration of the reactants system. During the preparation, 50 ml of a hydrochloric acid solution was added to dilute the reactants, which allowed slow nucleation of TiO<sub>2</sub> and resulted in the formation of large single crystals. **Figure 3a** shows a typical SEM image of a TiO<sub>2</sub> single crystal with highly exposed {001} facets. Due to the large particle size, the facets of {001} and {101} are easily observed and distinguished in SEM. A tilted-view from 45° angle help to clearly observe the exposed {001} and {101} facets (**Fig. 3b**). **Figure 3c** shows layered substructures on the {001} facet. It indicates an unexpected growth mechanism for the formation of {001} facets on TiO<sub>2</sub> single crystals. By changing the hydrothermal reaction temperature, the size of the TiO<sub>2</sub> single crystal can be easily controlled from 1 μm to 5 μm (**Fig. 3d**).

#### 3.3 TiO<sub>2</sub> mesoscopic assemblies

We also synthesized higher-level mesoscopic assemblies from TiO<sub>2</sub> nanocrystals with exposed high

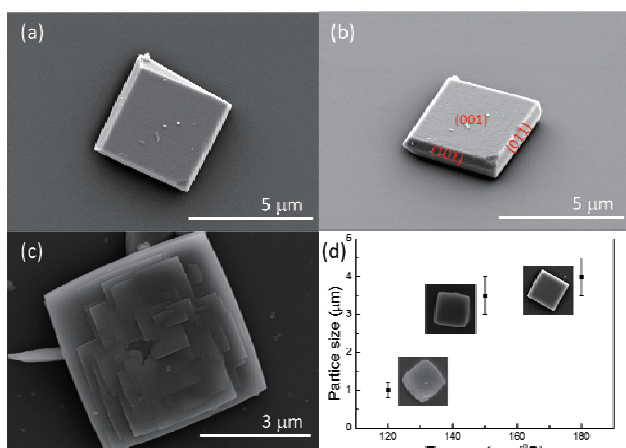


**Fig. 3** SEM photographs of TiO<sub>2</sub> single crystal with exposed {001} facets from top-view (a) and 45° tilted-view (b), and layered structure on the {001} facet (c). A relationship between particle size and hydrothermal temperature (d).

energy {001} facets, which are expected to offer some superior performance in lithium ion battery and dye-sensitized solar cells<sup>10,11</sup>. **Figure 4** shows four kinds of TiO<sub>2</sub> mesoscopic assemblies prepared under different hydrothermal conditions. The mesoscopic solid TiO<sub>2</sub> microspheres consisting of many ultrathin {001} dominant TiO<sub>2</sub> sheets on the outer surfaces of microspheres were synthesized in a hydrochloric acid solution (1 M) with low reactant concentrations (**Fig. 4a**). The {001} facets on the outer surface of TiO<sub>2</sub> microspheres were developed when the concentration of hydrochloric acid solution was increased to 2 M and 5 M (**Figs. 4b and 4c**). This fact indicates that the acidic condition plays a critical role in the nucleation and crystal growth of TiO<sub>2</sub> microspheres. The rates of nucleation and crystal growth of TiO<sub>2</sub> sheets were further slowed down in the presence of surfactant (SDS), and resulted in the higher-level mesoscopic assemblies of TiO<sub>2</sub> microcrystals with well-developed {001} facets (**Fig. 4d**).

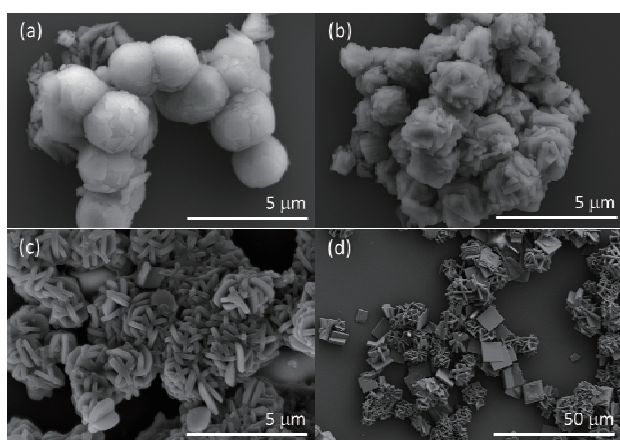


**Fig. 4** SEM photographs of highly-level mesoscopic microspheres assembly prepared in hydrochloric acid with concentration of 1 M (a), 2 M (b), 5 M (c), and prepared in the presence of surfactant SDS (d).

### 3.4 TiO<sub>2</sub> hollow microspheres

Synthesis of TiO<sub>2</sub> hollow microspheres were achieved by a modified hydrothermal method. Phthalic acid was used as a coupling agent to assemble the hydroxyl-terminal TiO<sub>2</sub> clusters into spherical aggregations in methanol medium. After aging for 1 hour in the hydrothermal condition, TiO<sub>2</sub> cluster aggregations changed to hollow microspheres. **Figure 5a** shows a typical TEM photograph of as-synthesized TiO<sub>2</sub> hollow microspheres obtained at 150 °C hydrothermal treatment. The particle size of hollow TiO<sub>2</sub> is about 500 nm with a shell thickness of 150 nm (**Fig. 5b**). When TiO<sub>2</sub> cluster aggregations were aged at 250 °C, big TiO<sub>2</sub> hollow microspheres were obtained (**Fig. 5c**). The as-prepared TiO<sub>2</sub> microspheres have an average size of 1.2 μm with a shell thickness of about 100 nm (**Fig. 5d**). The increase of particle size may be due to the increasing swelling pressure under high temperature. **Figures 5e-5h** show EDX element mapping of TiO<sub>2</sub> hollow microspheres. C signal is strong (15.5% content determined by element analysis) and homogeneous distribution in TiO<sub>2</sub> hollow microspheres, which due to phthalic acid acting as a coupling agent on the surface of TiO<sub>2</sub> clusters.

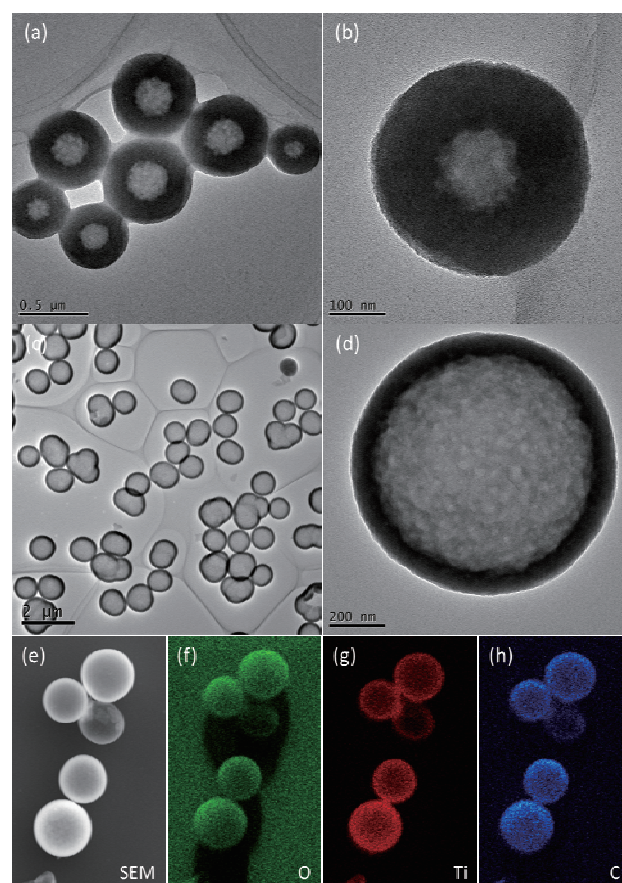


**Fig. 5** TEM photographs of TiO<sub>2</sub> hollow microspheres prepared at 150 °C (a, b) and 250 °C (c, d). EDX element mapping of TiO<sub>2</sub> hollow microspheres (e-h).

### 4. Conclusions

Size and morphology control are very important for

## Hydrothermal Synthesis and Morphology Control of TiO<sub>2</sub> Nanocrystals

the use in many fields because they play critical roles in the photocatalytic activity and other properties of nanostructured TiO<sub>2</sub>. In this study, we succeeded in the synthesis of size-controlled anatase TiO<sub>2</sub> nanosheets and single crystals with highly exposed {001} facets. The particle size is easily controlled ranging from 20 nm to several micrometers by carefully adjusting the F/Ti ratio and other parameters during the hydrothermal process. We also succeeded in morphology control of TiO<sub>2</sub> nanocrystals by hydrothermal method. Nanostructured TiO<sub>2</sub> are synthesized by selecting the hydrothermal conditions, including regular nanosheets, mesoporous nanosheets, highly-level mesoscopic microspheres assembly, and hollow microspheres. These size- and morphology-controlled nanostructured TiO<sub>2</sub> show great potential for applications in photocatalysts, dye-sensitive solar cells, gas sensors, and bio-medical applications.

### Acknowledgements

The authors would like to thank the Advanced Low Carbon Technology Research and Development Program (ALCA) of Japan Science and Technology Agency for financial support. This work was also partly supported by a Grant-in-Aid for Cooperative Research Project of Advanced Materials Development and Integration of Novel Structured Metallic and Inorganic Materials and for Scientific Research from the Ministry of Education, Culture, Sports, Science and Technology of Japan.

### References

- 1) X. Chen and S. S. Mao, *Chem. Rev.* 107 (2007) 2891-2959.
- 2) G. Liu, J. C. Yu, G. Q. Lu and H. M. Cheng, *Chem. Commun.* 47 (2011) 6763-6783.
- 3) A. Selloni, *Nat. Mater.* 7 (2008) 613-615.
- 4) H. G. Yang, C. H. Sun, S. Z. Qiao, J. Zou, G. Liu, S. C. Smith, H. M. Cheng and G. Q. Lu, *Nature* 453 (2008) 638-642.
- 5) X. Han, Q. Kuang, M. Jin, Z. Xie and L. Zheng, *J. Am. Chem. Soc.* 131 (2009) 3152-3153.
- 6) N. Murakami, Y. Kurihara, T. Tsubota and T. Ohno, *J. Phys. Chem. C* 113 (2009) 3062-3069.
- 7) Q. Wu, M. Liu, Z. Wu, Y. Li and L. Piao, *J. Phys. Chem. C* 116 (2012) 26800-26804.
- 8) C. B. Almquist and P. Biswas, *J. Catal.* 212 (2002) 145-156.
- 9) Z. Tan, K. Sato, S. Takami, C. Numako, M. Umetsu, K. Soga, M. Nakayama, R. Sasaki, T. Tanaka, C. Ogino, A. Kondo, K. Yamamoto, T. Hashishin, S. Ohara, *RSC Adv.* 3 (2013) 19268-19271.
- 10) S. W. Liu, J. G. Yu and M. Jaroniec, *J. Am. Chem. Soc.* 132 (2010) 11914-11916.
- 11) Q. J. Xiang, J. G. Yu and M. Jaroniec, *Chem. Commun.* 47 (2011) 4532-4534.